IEEE Access
Multidisciplinary ⋮ Rapid Review ⋮ Open Access Journal

Received September 1, 2021, accepted September 5, 2021, date of publication September 7, 2021,
date of current version September 17, 2021.

Digital Object Identifier 10.1109/ACCESS.2021.3111006

Single Value Decomposition to Estimate Critical Clearing Time of a Power System Using Measurements

MARTHA N. ACOSTA[1], EDGAR GÓMEZ[2], FRANCISCO GONZALEZ-LONGATT[1], (Senior Member, IEEE), MANUEL A. ANDRADE[2], (Member, IEEE), ERNESTO VÁZQUEZ[2], (Member, IEEE), AND EMILIO BAROCIO[3], (Senior Member, IEEE)

[1]Department of Electrical Engineering, Information Technology and Cybernetics, University of South-Eastern Norway, 3918 Porsgrunn, Norway
[2]School of Mechanical and Electrical Engineering, Universidad Autónoma de Nuevo León, San Nicolás de los Garza, Nuevo León 66451, Mexico
[3]Electrical Engineering Department, Universidad de Guadalajara, Guadalajara, Jalisco 44100, Mexico

Corresponding author: Francisco Gonzalez-Longatt (fglongatt@fglongatt.org)

ABSTRACT The transient stability analysis of large-interconnected power systems using time-domain simulations (TDS) is a significant challenge since it represents a huge computational cost. Besides, for dynamic security assessment is required have a quick response. Consequently, recent approaches are relying on using the wide-area measurement system combined with other techniques to perform transient stability assessment and counteract the drawbacks of the TDS method. However, these approaches still requiring to perform TDS to set initial parameters. This paper proposes a new algorithm to estimate the critical clearing time (CCT) based on the eigenvalue calculation and the singular value decomposition using data from wide-area measurement systems. The proposed algorithm uses the phase angles of the voltage phasors measurements at the generation buses to represent the dynamics of the internal angles of the generators. First, from a set of signals, a measurement matrix is formed using a sliding window. Then, a threshold based on the maximum singular value and the dominant eigenvalue of the measurement matrix are computed. Finally, the CCT is estimated using the dominant eigenvalue (the most energetic eigenvalue) and the threshold. The proposed algorithm is evaluated using the Kundur four-machine system and New England 39-Bus system. Its performance contrasts to the CCT calculated using the classical TDS. The simulation results demonstrated acceptable precision of the CCT against TDS. Also, it presents robustness against the effect of the noise in the measurements. Therefore, it is suitable for online applications.

INDEX TERMS Critical clearing time, eigenvalues, energy function, lyapunov function, power system stability, single value decomposition, WAMS.

I. INTRODUCTION

Transient power angle stability is concerned with the ability of the power system to maintain synchronism when subjected to a severe disturbance, such as a short circuit on a transmission line [1], [2]. The post-disturbance transient stability assessment allows the network operators to take emergency control actions and avoid instability [3], [4]. In the transient stability assessment (TSA), the critical clearing angle is defined as the switching angle for which the system is at the edge of instability. In other words, the synchronous generator is destined to become unstable if the fault is not cleared by the time the synchronous generator reaches the critical clearing angle, so-called critical clearing time (CCT) [5].

The importance of calculating the CCT of a given fault is directly related to the capability of the power system to transfer power, i.e., every millisecond saved in fault clearing time (FCT) means more power can be transferred. For instance, Eastvedt in [6] shows that a one-cycle reduction in FCT on a particular transmission line for a specific power system increased the power transfer by 250 MW, amounting to about 15 MW per millisecond (see Figure 1).

Recent methods still using traditional techniques, such as time-domain simulation (TDS) or sensitivity of parameters,

The associate editor coordinating the review of this manuscript and approving it for publication was Qiuye Sun.

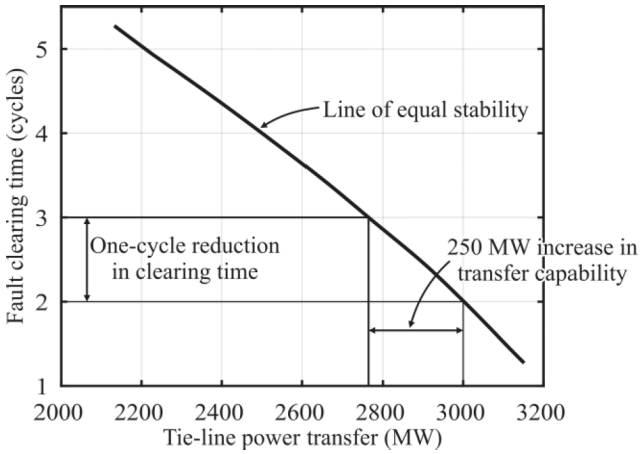

FIGURE 1. An illustrative example of the relation between the fault clearing time (FCT) and the power transferred, at 60 Hz., by Eastvedt [6].

to compute the CCT. For instance, [7] proposes a method to derive an exact equation for the first-order sensitivity of the critical clearing time concerning any system parameter. However, new methods have assumed using the wide-area measurement system (WAMS) as an advantage in TSA and calculating the CCT of a fault. These methods use the measurement of electrical variables instead of modelling the power system by the DAEs [8]–[13]. In this sense, [14] introduces a method to calculate CCT by computing the fault-on trajectory at the stability boundary. The critical synchronous generator is determined, and the least square minimisation is computed to obtain the CCT.

Furthermore, [15] introduces a study where the whole power system is represented with a single machine equivalent model, and its parameters are estimated using online measured data. Then, a graphical index, based on the transient energy approach, is introduced to estimate the transient stability limit. While [16] proposes a non-parametric statistic scheme to evaluate the stability margin online. This method needs off-line learning that requires a database of operating conditions and TDS to obtain 14 kinds of indicators and a stability margin.

In addition to the use of WAMS, several methods have adopted the singular value decomposition (SVD) technique and other closely related methods, such as principal component analysis (PCA) and proper orthogonal decomposition (POD). These techniques were implemented to analyse the information of a high dimensional dataset and project it onto a lower-dimensional space, with a minimum loss of information [17], [18]. One of the first applications of these methodologies in electric power systems is in voltage stability assessment. SVD method has been used as a voltage security index by examining the smallest singular value of the Jacobian [19]. Moreover, recently SVD has been used to analyse the information of the inverse Jacobian matrix to identify the most sensitive buses of the power system by obtaining the most significant singular values [20].

Meanwhile, in TSA, empirical orthogonal functions based on POD are applied to extract dynamic patterns and phase relationships among critical modes from WAMS [21]. Also, it is combined with Hilbert analysis to extract the dominant modes of oscillations [22], [23]. First, the empirical mode decomposition has been used to extract modal components of voltage and frequency. Then, the two-machine system equivalent model is used to estimate the CCT [24]. Finally, PCA is applied to detect and extract unusual dynamic events from measured data [25]. The POD and Hilbert analysis approach is also used to determine the characteristics of the torsional shaft signals [26]. Moreover, the SVD method has been used to identify and form coherent groups [27], [28].

On the other hand, the random matrix theory has become a subject of study and application for a wide range of disciplines. But it is specially used for multivariate data analysis. This methodology mainly follows two approaches: assuming asymptotic convergence with infinite matrix size and non-asymptotic convergence considering finite matrix size. The application of random theory in power systems has been growing; for instance, [29] uses random matrix theory to create a framework for data-driven of smart grids for power flow analysis and fault detection. Moreover, in [30], this technique was used to detect events in the power system.

Even though the mentioned methods avoid computing the DAEs, which describe the power dynamics, and meet the objective of performing a transient stability assessment and obtaining the CCT of a fault. Some methods, such as [7]–[16], require TDS information to set limits to evaluate energy equations, increasing the computational burden. Likewise, some others require knowing network topology and power system parameters such as the impedance of the transmission lines, inertia, and synchronous generators damping, leading to low accuracy of the CCT when the system parameters are unknown. Finally, other methodologies, such as [15], [24], require representing the entire power system into a single machine equivalent model, overlooking relevant information of the power system. These drawbacks grow the need to develop new methodologies to estimate the critical clearing time of a fault.

The main objective of this research paper is to take advantage of the measurements coming from the WAMS to perform transient stability assessment without performing the DAEs or requiring the system parameters. It proposes an algorithm to estimate the CCT of the power system based on the computation of the eigenvalues and the SVD of spatial-temporal data coming from WAMS. First, the proposed algorithm takes the electromechanical variables measured from WAMS to construct a measurement matrix using a sliding window. Then SVD technique is computed to extract the main features of the measurement matrix and determine the range of variation of the eigenvalues concerning the changes in the power system. Afterwards, the maximum singular value is used to establish the variation limit of the eigenvalues of the measurement matrix. This variation limit is used to determine whether the power system remains under stable operating

conditions or unstable after a disturbance occurs. Moreover, the information provided by the eigenvalue angle can be used to determine whether the power system has a disturbance. Finally, the maximum eigenvalue of the measurement matrix and the variation limit are used to compute the CCT.

The significant contributions unfolding from this paper are listed below:

1) An algorithm to compute the CCT of a power system based on measurements is proposed. It does not require knowing the power system parameters, creating a model or computing the DEAs. It instead captures the main characteristics of the system dynamics using WAMS.
2) The proposed methodology uses the measurements of voltage angle phasor instead of frequency, demonstrating suitability for stability assessment.
3) Two conditions to identify whether the system is stable or unstable after a disturbance are defined based on the Lyapunov surface and the most energetic eigenvalue of the measurement matrix.
4) The proposed methodology is suitable for online applications since the computational burden required to compute the eigenvalues and singular values are low.
5) The algorithm to compute the CCT is not affected by the inherent noise of the measurements.

This paper is organised as follows: A review of the SVD, covariance matrix and Lyapunov-type function are presented in Section II. A discussion of the characteristics of the maximum singular values and the eigenvalues of a measurement matrix and its interpretation is given in Section III. Also, it describes the procedure used to create the measurement matrix from a sliding window using measurements of electromechanical variables measured from WAMS. The proposed algorithm is fully explained in Section IV, followed by its application for three test systems with simulation results presented in Section V. Also, a discussion of the main contributions is introduced in Section VI. Finally, the conclusion is given in Section VII.

II. MATHEMATICAL FOUNDATION

A. SINGULAR VALUES DECOMPOSITION

For a real measurement matrix, $\mathbf{X} \in \mathbb{R}^{m\times n}$, with rank r ($m \geq n$ and $r \leq n$), there exist orthogonal matrices $\mathbf{U} \in \mathbb{R}^{m\times m}$ and $\mathbf{V} \in \mathbb{R}^{n\times n}$ such that

$$\mathbf{X} = \mathbf{U}\mathbf{S}\mathbf{V}^{\mathrm{T}} \tag{1}$$

where $\mathbf{V}^{\mathrm{T}}$ is the conjugate transpose of $\mathbf{V}$ and $\mathbf{S}$ is a pseudo-diagonal and semidefinite matrix. The columns of $\mathbf{U}$ are called the left singular vectors, the rows containing the elements of the right singular vectors, and $\mathbf{S}$ contains the singular values denoted as $\sigma_1, \sigma_{1,\ldots,}\sigma_r$. Furthermore, $\sigma_k > 0$ for $1 \geq k \geq r$ and $\sigma_k = 0$ for $(r+1) \geq k \geq n$ [31].

Generally, singular values reveal how much stretch or compress can present an eigenvector under a transformation by an arbitrary matrix. Therefore, the matrix $\mathbf{X}$ maps a unit sphere in m dimension space to an ellipsoid in r dimension space with the directions indicated by left singular vectors and magnitudes of singular values. The angle projection β is the angle between the x_1-axis and the new u_1-axis; since the projection is orthogonal, the angle between the maximum singular value and the rest of the singular values (α) is $\pi/2$ rad. Moreover, the maximum singular value of matrix $\mathbf{X}$ is the Euclidean norm of the matrix [32]. To illustrate this, the mapping for a matrix of $m = 3$, $n = r = 2$ and the maximum singular value are shown in Figure 2.

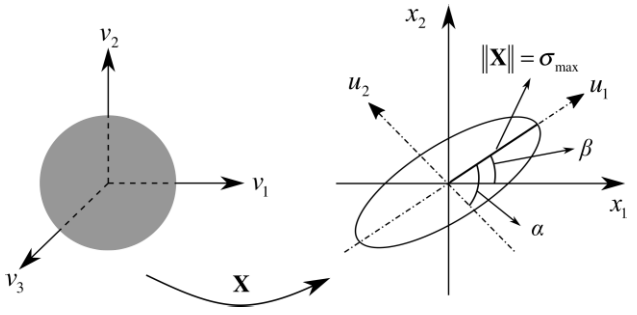

FIGURE 2. Geometric interpretation of SVD mapping.

B. COVARIANCE MATRIX

Let $\mathbf{X} \in \mathbb{R}^{m\times n}$ be a matrix containing a set of data discretised in space and time, where m is the number of samples and n is the number of observations. The covariance matrix of $\mathbf{X}$ is defined as [18]:

$$\mathbf{C} = \frac{1}{m}\sum_{\substack{i=1\\ j=1}}^{n} (\mathbf{x}_i - \bar{\mathbf{x}}_i)^{\mathrm{T}}(\mathbf{x}_j - \bar{\mathbf{x}}_j) \tag{2}$$

where $\mathbf{C}$ is an $n \times n$ symmetric positive definite matrix and $\bar{\mathbf{x}}$ represents the mean of the vector $\mathbf{x}$. Assuming the data have a zero mean, the sample covariance is given by the following expression:

$$\mathbf{C} = \frac{1}{m}\mathbf{X}^{\mathrm{T}}\mathbf{X} \tag{3}$$

and can be diagonalised as

$$\mathbf{C} = \mathbf{V}\mathbf{D}\mathbf{V}^{\mathrm{T}} \tag{4}$$

where $\mathbf{D}$ is a diagonal matrix containing the eigenvalues denoted as $\sigma_1, \sigma_{1,\ldots,}\sigma_r$. The columns of $\mathbf{V}$ and $\mathbf{V}^{\mathrm{T}}$ contain the right and left eigenvectors, respectively.

C. LYAPUNOV-TYPE FUNCTIONS

Consider the linearised system described by

$$\dot{x} = \mathbf{A}x \tag{5}$$

A quadratic function

$$V(x) = x^{\mathrm{T}}\mathbf{P}x = \sum_{i=1}^{n}\sum_{j=1}^{n} p_{ij}x_i x_j \tag{6}$$

is a Lyapunov-type function if the matrix $\mathbf{P}$ is positive definite. Moreover, the derivative of (6) along the trajectories of (5) is defined as

$$\dot{V}(x) = x^{\mathrm{T}}\mathbf{P}\dot{x} + \dot{x}^{\mathrm{T}}\mathbf{P}x = x^{\mathrm{T}}(\mathbf{PA} + \mathbf{A}^{\mathrm{T}}\mathbf{P})x = -x^{\mathrm{T}}\mathbf{Q}x \quad (7)$$

where $\mathbf{Q}$ is a real symmetric matrix definite by $\mathbf{PA} + \mathbf{A}^{\mathrm{T}}\mathbf{P} = -\mathbf{Q}$ and the origin is asymptotically stable if Q is positive definite [33].

III. MATHEMATICAL FORMULATION

A critical aspect of an appropriate TSA is an accurate and suitable model of the power system that contains the information of the network topology and the electromechanical parameters of the power systems elements. At present, having a realistic full-detailed model of the power system represents a significant challenge due to the constant change of the network topology, the dynamics and uncertainties related to the loads and the high complexity and non-linearity of the models used in some power system devices, e.g., FACTS.

The emergence of WAMS offers advantages for analysing the transient stability of the power system, e.g., the analysis becomes more precise and decreases the computational burden [9], [34]. However, due to the difficulty of measuring the angle and frequency of the rotor in a real power system, it is considered that the voltage phasor angle dynamics in the generation buses, obtained from WAMS, is representative of the dynamics of the internal angle of the synchronous generator, this in terms of the response to a disturbance (see Figure 3) [22].

Therefore, in this paper, the set of variables obtained from WAMS are the voltage phasors measured at the generation buses, and there are required two kinds of measurements:

1) A set of reference signals: Set of signals for a stable condition operation; this measurement is taken only once to establish a reference of operation.
2) A set of working signals: This set of signals for any operating condition of the power system.

A. MEASUREMENT MATRIX

The measurement matrix, $\mathbf{X} \in \mathbb{R}^{m\times n}(m > n)$, containing the angles of the voltage phasors obtained from WAMS, is constructed using an m-sample sliding window, where m is the number of samples of the sliding window and n is the number of observed variables. This matrix is formed by vectors, $\mathbf{x}_i = [x(\theta_i, t_1)x(\theta_i, t_2)\ldots x(\theta_i, t_m)]^{\mathrm{T}}$, $i = 1,2,\ldots,n$, which represent a set of snapshots obtained from the i-th observed variable and $t_1, t_2, \ldots, t_m$, is the time at which the observations are made. The set of data can be written as [21]:

$$\mathbf{X} = \begin{bmatrix} \mathbf{x}_1 & \mathbf{x}_2 & \cdots & \mathbf{x}_n \end{bmatrix} = \begin{bmatrix} x(\theta_1, t_1) & \cdots & x(\theta_n, t_1) \\ \vdots & \vdots & \vdots \\ x(\theta_1, t_m) & \cdots & x(\theta_n, t_m) \end{bmatrix} \quad (8)$$

The set of spatial-temporal data that capture the main characteristics of the system dynamics can be analysed by

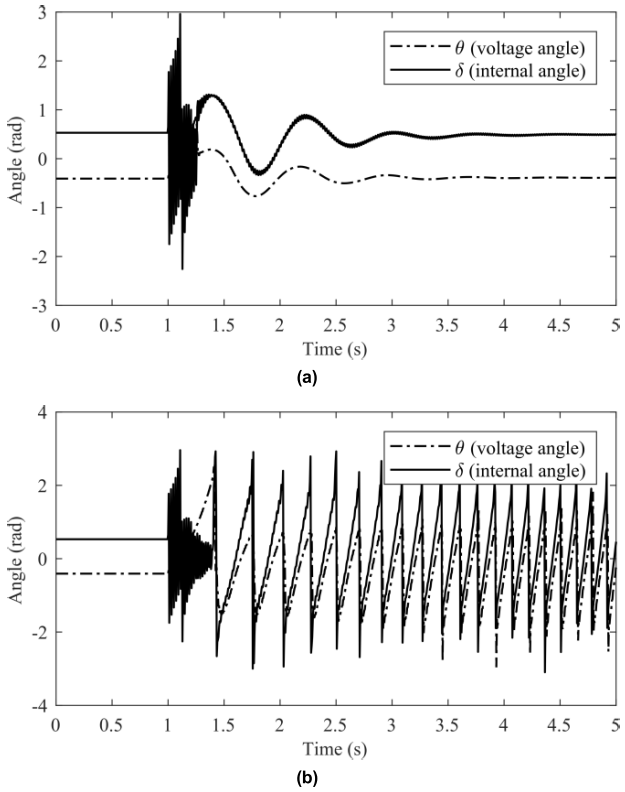

FIGURE 3. Dynamic behaviour of the estimated internal angle of the synchronous generator (δ) and voltage phasor angle (θ) measured at the generation bus for a three-phase fault: a) Stable case, b) Unstable case.

different techniques, e.g., empirical orthogonal function analysis [21], [25]. The primary objective of these techniques is extracting the information from the data set by projecting the data in the low space.

To map out the data of the measurement matrix, $\mathbf{X}$, into a low dimension space and extract the main information, the SVD can be computed; another way is computing the covariance matrix. Both procedures are of interest since computing (1) allows obtaining the maximum stretch that the eigenvector of the matrix $\mathbf{X}$ can be experienced by computing the maximum singular value $\sigma_{\max}$. Meanwhile, computing the covariance matrix for a set of discretised data brings information about the eigenvalues of $\mathbf{X}$. Therefore, the definition of the singular value decomposition given in (1) is used to establish a relationship between the eigenvalues of a covariance matrix and the singular values of a matrix. This relationship is mathematically represented as follow

$$\mathbf{X}^{\mathrm{T}}\mathbf{X} = \left(\mathbf{USV}^{\mathrm{T}}\right)^{\mathrm{T}}\left(\mathbf{USV}^{\mathrm{T}}\right) = \mathbf{VS}^2\mathbf{V}^{\mathrm{T}} \quad (9)$$

According to (9), the right singular eigenvectors of $\mathbf{X}$ are right eigenvectors of $\mathbf{X}^{\mathrm{T}}\mathbf{X}$. Moreover, the singular values of $\mathbf{X}$ are found to be the square roots of the eigenvalues of $\mathbf{X}^{\mathrm{T}}\mathbf{X}$. Now, using this deduction and substituting (9) in the equation (3), the covariance matrix, $\mathbf{C}$, can be expressed in

terms of the singular values of the $\mathbf{X}$, such as

$$\mathbf{C} = \frac{1}{m}\mathbf{X}^{\mathrm{T}}\mathbf{X} = \frac{1}{m}(\mathbf{V}\mathbf{S}^2\mathbf{V}^{\mathrm{T}}) \tag{10}$$

and it is easy to see that the i-th eigenvalue (λ_i) of $\mathbf{C}$ is related to the i-th singular value (σ_i) as follows

$$\sigma_i = \sqrt{m\lambda_i} \tag{11}$$

On this basis, in this paper, the information of the measurement matrix, $\mathbf{X}$, will be extracted by computing the covariance matrix using (3) and then $\mathbf{C}$ is diagonalised as in (4). The maximum singular value ($\sigma_{\max}$), i.e., the singular value related to the dominant eigenvalue, is obtained by using (11). The energy of the i-th eigenvalue can be estimated $E_i = \lambda_i \Big/ \sum_{j=1}^{n} \lambda_j$ [22]. The eigenvalue of the matrix that contains about 99% of the average energy is called the dominant eigenvalue (λ_d).

B. POWER SYSTEM ENERGY FUNCTION

Analogous to Lyapunov's theory, power system stability can be evaluated regarding energy since the kinetic energy of the turbines and the potential energy stored in the inductive branches can be represented as a power system energy function. Moreover, this energy function is always decreasing in time due to the damping in the turbines; this characteristic provides the most natural certificate of local stability [2].

In [35], it is proved that a Lyapunov-type function can be constructed from the eigenvectors of a matrix, and it is interpreted as the energy stored in the eigenvalues of this matrix. Since this paper proposes only using measurements obtained from WAMS and the system is conservative, the measurements can directly express the energy. Hence, if a Lyapunov-type function is written using only the measurements, it can be expressed as

$$V(x) = x^{\mathrm{T}}(\tilde{v}\tilde{v}^{\mathrm{T}})x \geq 0 \tag{12}$$

where $\tilde{v}$ is the left eigenvector corresponding to λ_d of the matrix $\mathbf{C}$ from (3). Let $V(x) = T_\lambda$ be a Lyapunov surface for some $T_\lambda > 0$. Since matrix $\mathbf{C}$ is positive definite, the condition in (6) holds, and $V(x) \to T_\lambda$ as $t \to \infty$. Furthermore, knowing that $\mathbf{C}$ is positive definite and hence all its eigenvalues are positive, the equation (7) can be evaluated by

$$\dot{V}(x) = \lambda_d V(x) \leq T_\lambda \tag{13}$$

Now, to prove that (13) holds, it is needed to show that the energy stored in the dominant eigenvalue is decreasing after a disturbance, i.e., $\lambda_d(t) \to \lambda_d(t_0)$ as $t \to \infty$, where $\lambda_d(t_0)$ is the energy stored in dominant eigenvalue in the pre-fault period. Since the Lyapunov surface, $V(x) \to T_\lambda$, represents the boundary of stability in terms of energy, i.e., the boundary of energy that the power system can dissipate after a disturbance, and $\lambda_d(t)$ represents the energy of the power system in each moment. Based on the Lyapunov surface and the dominant eigenvalue, two conditions to identify whether the system is stable or unstable after a disturbance are defined:

Condition 1: If $\lambda_d(t) \leq T_\lambda$ when $t \to \infty$, the power system will be stable.

Condition 2: If $\lambda_d(t) > T_\lambda$ when $t \to \infty$, the power system will be unstable.

The above conditions can be illustrated in Figure 4. Once the fault-on period begins, the system is gaining energy. As more energy is gained, $\lambda_d(t)$ approaches to the boundary T_λ. The post-fault period starts when the fault is cleared, and the energy stored in the dominant eigenvalue at this time is represented by $\lambda_d(t_{\mathrm{cl}})$. Analogous to equal area criterion [36], when $\lambda_d(t_{\mathrm{cl}})$ does not reach T_λ, the energy will be dissipated and $\lambda_d(t_{\mathrm{cl}}) \to \lambda_d(t_0)$. Otherwise, if $\lambda_d(t_{\mathrm{cl}})$ overcomes T_λ, all the energy gained in the fault-on period cannot be dissipated, and $\lambda_d(t_{\mathrm{cl}})$ cannot go back inside $V(x) = T_\lambda$. Additionally, the critical clearing time, τ, is such time that makes λ_d be at the boundary of T_λ and it tends to leave $V(x) = T_\lambda$.

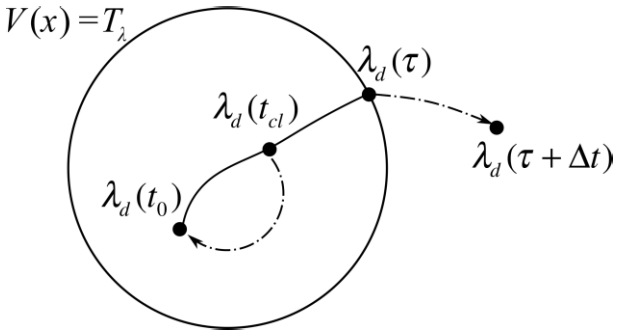

FIGURE 4. Visualisation of the energy of the power system as a function of the dominant eigenvalue, λ_d.

IV. PROPOSED METHODOLOGY: CCT CALCULATION BASED ON SVD

The proposed algorithm to estimate the CCT using SVD is based on calculating a threshold that represents the energy that can dissipate the power system and the observation of the dominant eigenvalue. For each m-sample sliding window, a measurement matrix ($\mathbf{X}$) is formed as described above, and then the covariance matrix, $\mathbf{C}$, is calculated. The covariance matrix is used to extract the dominant eigenvalue and the maximum singular value of the measurement matrix. First, $\sigma_{\max}$ is used to compute a threshold and set a boundary of energy. Then, λ_d is observed in each sliding window. If a disturbance occurs, λ_d is compared to the threshold. If the dominant eigenvalue crosses the threshold, the algorithm computes the CCT.

The proposed algorithm to estimate the CCT is performed in two stages, and it is summarised in Figure 5.

A. STAGE 1: PROCEDURE TO TUNE THE THRESHOLD

From the definition of the SVD, it is deducted that the maximum singular value of a matrix expresses the maximum energy that can take its associated eigenvalue. In this paper, the energy of the power system is represented by the energy

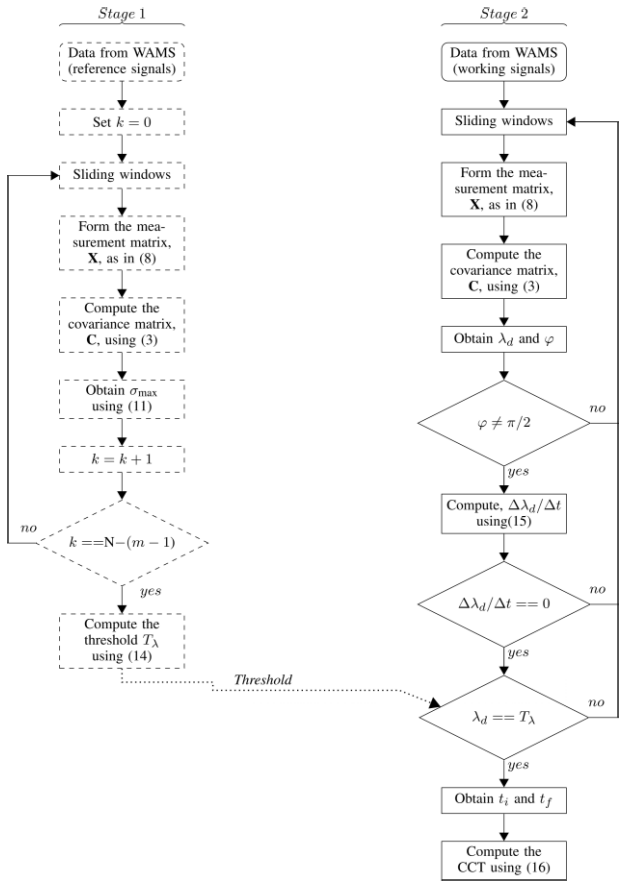

FIGURE 5. Flowchart of the proposed algorithm of the estimation of CCT by using SVD.

of the dominant eigenvalue. Hence, to compute the boundary of energy that the system can be dissipated, the maximum singular value, $\sigma_{\max}$, is used for the un-faulted steady-state operation (reference signals) to estimate a threshold T_λ. Furthermore, the threshold is used to estimate the CCT and as a limit of stability.

The maximum energy that the eigenvalue of a measurement matrix can take ($\sigma_{\max}$) is defined by (11); this value is used to compute a threshold. The threshold can determine if the power system is stable after a disturbance by evaluating Condition 1 and Condition 2 establish in Section III.B.

The set of reference signals of N-sample are used to compute the threshold (T_λ), and the procedure is summarised as follows:

1) From a set of reference signals containing the angles of the voltage phasors measured at the generation buses (θ_{01}, $\theta_{02}, \ldots, \theta_{0n}$), form a measurement matrix, **X**, as in (8).
2) Compute the covariance matrix, **C**, using (3).
3) Obtain the maximum singular value ($\sigma_{\max}$) of **C** using (11).
4) Repeat steps 1) and 2) along the entire reference signal.
5) Identify if all the maximum singular values ($\sigma_{\max,i}$) are obtained, i.e., when $k = N - (m-1)$, where N is the number of samples of the reference signal and m is the number of samples of the sliding window.
6) Compute the threshold as follows:

$$T_\lambda = \frac{1}{k}\sum_{i=1}^{k} \sigma_{\max i} \tag{14}$$

This stage is only run once unless the parameters or the topology of the power system are changed. In this case, the threshold should be recalculated. The value of T_λ will be used in Stage 2.

B. STAGE 2: CALCULATION OF THE CCT

Since T_λ represents the maximum energy that the power system can dissipate and is based on the behaviour of the angles in steady-state operation, the energy of λ_d is less than T_λ when the power system is in steady-state operation. Moreover, when the power system is disturbed, the energy of λ_d takes larger magnitudes, which may or may not be below the limit established by T_λ as this will depend on the type of disturbance and its duration. Therefore, after a disturbance, if the magnitude of λ_d is less than T_λ, Condition 1 is fulfilled, ensuring that the power system remains stable. In contrast, if λ_d takes magnitudes larger than T_λ, then Condition 2 is fulfilled, and the power system will be unstable.

As mentioned above, the projection of a matrix into a low dimensional space is orthogonal. Then, the angle between the maximum singular value and the rest of the singular values is $\pi/2$ rad; this is shown in Figure 2. Hence, it is analogous to observe the angle between λ_d and the rest of the eigenvalues of matrix **C**. This angle is computed, making the sum of all eigenvalues different of λ_d as real part and λ_d as complex part, the angle of this complex number is φ, and it is given in radians. For the un-faulted power system, the angle between λ_d and the rest of the eigenvalues φ holds $\pi/2$ rad. However, whenever the power system has a disturbance $\varphi \neq \pi/2$.

Another essential characteristic to observe is the trajectory of λ_d. After a fault starting, it is crucial to detect the point in which the trajectory of λ_d change from concave to convex or vice versa. The λ_d trajectory change can be identified by computing the rate of change of λ_d as follows

$$\frac{\Delta\lambda_d}{\Delta t} = \frac{\lambda_{dk} - \lambda_{d(k-1)}}{\Delta t} \tag{15}$$

where k represents the current sliding window and k-1 is the previous sliding window. When $\Delta\lambda_{d,k}/\Delta t$ crosses zero means that the trajectory of λ_d has changed.

The CCT is determined as the time required for λ_d to cross the threshold measured from the onset of the fault, calculated as follows:

$$t_{\text{CCT}} = t_f - t_i \tag{16}$$

where t_i is the fault starting time determined when $\varphi \neq \pi/2$. After a change of trajectory, i.e., $\Delta\lambda_{d,k}/\Delta t = 0$, the time t_f is determined as the time when the magnitude of λ_d reaches the threshold calculated at Stage 1, i.e., when $\lambda_d = T_\lambda$.

The procedure to compute the CCT of a fault is summarised as follows:

1) From a set of working signals containing the angles of the voltage phasors measured at the generation buses ($\theta_1, \theta_2, \ldots, \theta_n$), form a measurement matrix, $\mathbf{X}$, as in (8).
2) Compute the covariance matrix, $\mathbf{C}$, using (3).
3) Obtain the dominant eigenvalue (λ_d) of $\mathbf{C}$ and obtain φ.
4) If $\varphi \neq \pi/2$ go to the next step. Otherwise, return to step 1).
5) Compute $\Delta\lambda_{d,k}/\Delta t$ using (15).
6) If $\Delta\lambda_{d,k}/\Delta t = 0$, go to the next step. Otherwise, return to step 1).
7) If $\lambda_d = T_\lambda$, go to the next step. Otherwise, return to step 1).
8) Obtain the fault starting time (t_i), i.e., the first time when $\varphi \neq \pi/2$.
9) Obtain the time t_f.
10) Compute the CCT of a fault using (16).

V. SIMULATION RESULTS

This section is dedicated to demonstrating the suitability of the proposed algorithm for calculating the CCT by using the SVD. A sampling frequency of 2.048 kHz was used along with a 256-sample sliding window. In addition, tree illustrative test systems are used for demonstrative purposes considering bolted three-phase fault as a disturbance.

The evaluation of the proposed algorithm performance is carried out by calculating the CCT using the algorithm and then is compared to that obtained from another method. The percentage of variation (ξ) on the CCT calculation is obtained by the following equation:

$$\xi = \frac{t_{\mathrm{CCT}} - t_{\mathrm{CCT0}}}{t_{\mathrm{CCT0}}} \times 100\% \tag{17}$$

where t_{CCT} is the time calculated by the proposed algorithm and t_{CCT0} is the time obtained by another method. A negative sign indicates an underestimation of the CCT, i.e., there is less time to take control actions based on the CCT. Otherwise, if the sign is positive, there is an overestimation of the CCT.

The time-domain simulation methodology is carried out to compute the baseline CCT (t_{CCT0}) of the test system I and test system III. Besides, the baseline CCT (t_{CCT0}) of test system II is computed using the methodology proposed in [24]. Afterwards, the performance of the proposed algorithm to compute the CCT is assessed by computing equation (17).

A. TEST SYSTEM I

The test system I consists of 6 generators, 27 buses, 11 transformers, 31 transmission lines and 15 loads. The nominal frequency of the system is 50 Hz, and the voltage level is 54 kV. Generator G1 represents the interconnection with the rest of the transmission system; it is used as a reference busbar modelled as a constant 400 kV voltage source. Besides, the transmission lines are represented by the π-model. The parameters and the system diagram are described in Appendix A.

The threshold of Test System I, calculated using (14) $N = 10241$ and $k = 9986$, is T_λ =0.9739. The behaviour of λ_d for the pre-fault system is practically constant at a value of 0.9483, without exceeding the threshold.

Eight simulation cases are defined to evaluate the proposed methodology. Each case considers the CCT calculated for the critical transmission lines (see Table 1). For each case, a bolted three-phase fault is applied to a transmission line, and the transmission line is disconnected to eliminate the fault; Case 8 is representative of Test System I.

TABLE 1. Results of calculation of the CCT of a fault for Test System I.

Case	Line	CCT (s)		
		TDS	Proposed CCT algorithm	ξ (%)
1	L2	0.338	0.336	−3.60
2	L3	0.550	0.351	−36.09
3	L15	0.329	0.328	−0.12
4	L17	0.329	0.324	−1.25
5	L26	0.325	0.287	−11.54
6	L21	0.325	0.322	−0.80
7	L26	0.359	0.356	−0.81
8	L15	0.349	0.315	−9.48

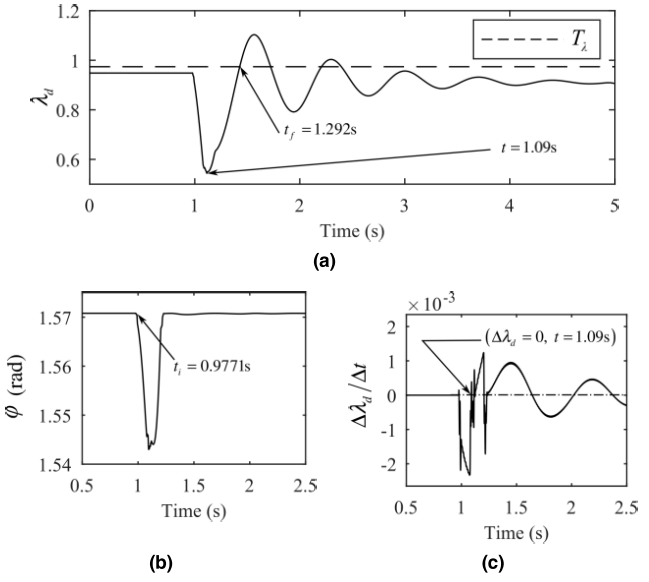

FIGURE 6. Time response of λ_d after a fault for a stable event (Test System I (Case8)): a) Magnitude of λ_d, b) Angle, φ, between λ_d and the rest of eigenvalues, c) Identification of λ_d trajectory change.

Case 8 is shown in Figure 6 for the faulted transmission line L15. The CCT calculate is t_{CCT} =0.315 s. The fault starting time is t_i =0.9771 s, and the λ_d trajectory change is detected at t = 1.09 s, which is the time at the trajectory of λ_d has the maximum amplitude. In this case, the magnitude of λ_d oscillates and stabilises below the threshold, so Condition 1 is fulfilled, and the power system is stable.

Table 1 presents a summary of the results obtained from the calculation of the CCT compared with those obtained by

TDS. The percentage of variation (ξ) obtained is also presented. For this test system, the results obtained for the CCT, using the proposed algorithm, are close to those obtained by TDS. The percentage of variation for all cases is negative, and the absolute mean of ξ is 7.96 %, and the CCTs obtained by the proposed method does not overcome those calculated by TDS. Therefore, it can be considered that the algorithm works correctly, and it is reliable.

B. TEST SYSTEM II: KUNDUR FOUR-MACHINE TEST SYSTEM

The two areas, Kundur four-machine test system, is used to evaluate the proposed algorithm. The nominal frequency of this test system is 50 Hz, and the voltage level is 230 kV. Area 1 contains generators 1 and 2 and transfers power through a tie line to area 2, which contains generators 3 and 4. The detailed model and the system parameter was obtained from [2], [24].

For this test system, a bolted three-phase fault was simulated at Bus 8 for various power transfer levels, and after a specific time, the fault is self-clearing.

The threshold of Test System II, calculated using (14) with N =10241 and k = 9986, is T_λ =0.4359. The behaviour of λ_d for the pre-fault system is practically constant at a value of 0.19, without exceeding the threshold.

Four cases are introduced to evaluate the proposed methodology for four levels of power transfer. Case 2 is representative of Test System II for a stable and unstable event.

Figure 7 shows Case 2 for a stable event. The level of power transfer for this case is 332 MW. The CCT calculate is t_{CCT} =0.325 s. The fault starting time is t_i =0.8755 s, and the λ_d trajectory change is detected at t = 1.082 s, which is the time at the trajectory of λ_d has the maximum amplitude.

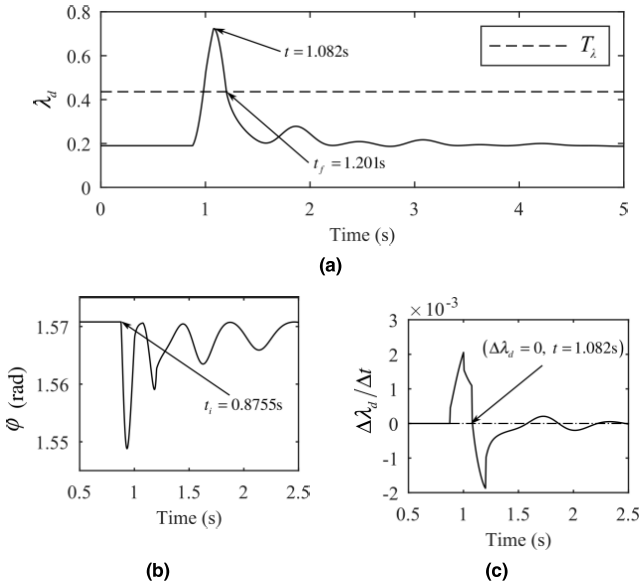

FIGURE 7. Time response of λ_d after a fault for a stable event (Test System II (Case 2)): a) Magnitude of λ_d, b) Angle, φ, between λ_d and the rest of eigenvalues, c) Identification of λ_d trajectory change.

In this case, the magnitude of λ_d has a damped oscillates and stabilises below the threshold, so Condition 1 is fulfilled, and the power system is found to be stable.

Otherwise, Case 2 for an unstable event is shown in Figure 8. For this case, the fault starting time is t_i =0.8755 s and the λ_d trajectory change is detected at t = 2.409 s. If it is compared the time when λ_d trajectory change with the CCT obtained for a stable event for Case 2, it is concluded that the power system will be unstable because t = 2.409 s exceeds the time of CCT estimated for a stable event. Moreover, the magnitude of λ_d does not cross the threshold, T_λ, therefore Condition 2 is fulfilled, and the power system is found to be unstable.

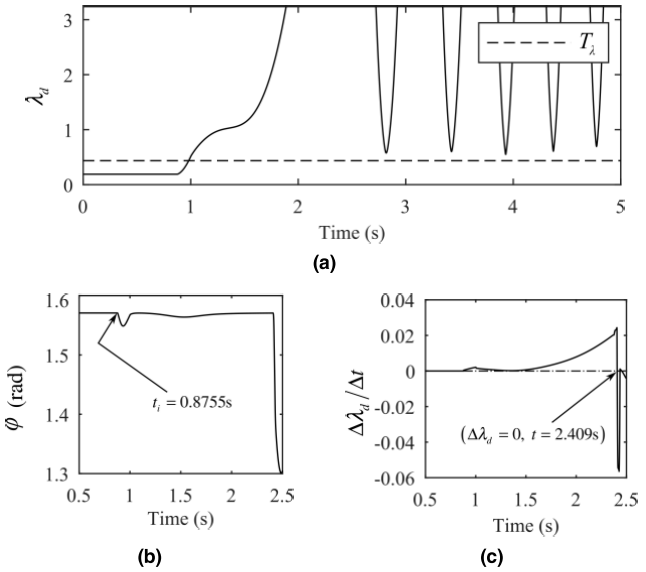

FIGURE 8. Time response of λ_d after a fault for an unstable event (Test System II (Case 2)): a) Magnitude of λ_d, b) Angle, φ, between λ_d and the rest of eigenvalues, c) Identification of λ_d trajectory change.

TABLE 2. Results of calculation of the CCT of a fault for Test System II.

Case	P(MW)	CCT (s)		
		Proposed by [24]	Proposed CCT algorithm	ξ (%)
1	232	0.585	0.500	−14.4
2	332	0.410	0.325	−20.6
3	432	0.230	0.215	−7.2
4	532	0.060	--	--

Table 2 presents a summary of the results obtained from the calculation of the CCT compared with those obtained by the method proposed in [24]. The percentage of variation obtained is also presented. For Case 4, the proposed algorithm does not estimate the CCT because the power transfer has increased considerably with respect to Case 1 and the threshold, T_λ, cannot be detected when λ_d crosses it. For this case,

T_λ must be recalculated, using (14), for the new steady-state operation.

C. TEST SYSTEM III: NEW ENGLAND 39-BUS SYSTEM

The New England 39-Bus system is used to evaluate the proposed algorithm. The detailed model and the system parameter was obtained from [37]. For this test system, a bolted three-phase fault is applied to a transmission line and the transmission line is disconnected to eliminate the fault.

For this test system, the threshold calculated using (14) $N = 10241$ and $k = 9986$ is T_λ 0.7734. The behaviour of λ_d for the pre-fault system is practically constant at a value of 0.0957, without exceeding the threshold. To appraise the proposed algorithm, five cases are defined. Each case considers the CCT calculated for the critical transmission lines.

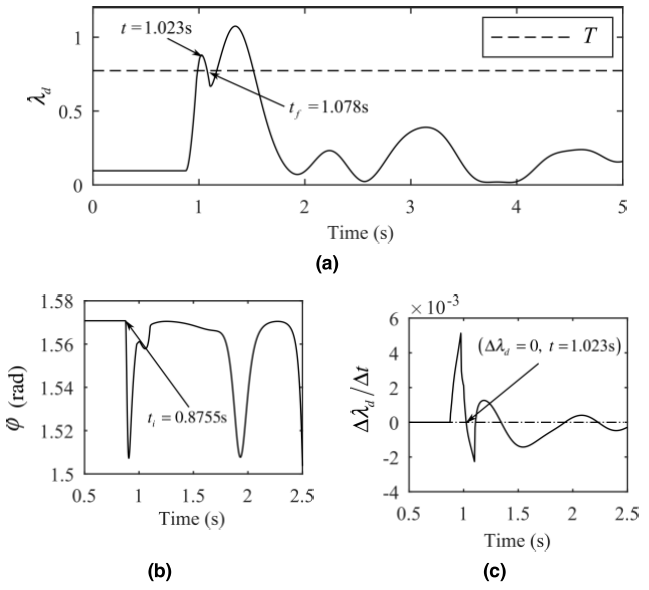

FIGURE 9. Time response of λ_d after a fault for a stable event (Test System III (Case 3)): a) Magnitude of λ_d, b) Angle, φ, between λ_d and the rest of eigenvalues, c) Identification of λ_d trajectory change.

Figure 9 shows Case 3 for a stable event. The estimated CCT is t_{CCT} =0.202 s. The fault starting time is t_i =0.8755 s, and the λ_d trajectory change is detected at $t = 1.023$ s, which is the time at the trajectory of λ_d has the maximum amplitude. In this case, the magnitude of λ_d has a damped oscillates and stabilises below the threshold, so Condition 1 is fulfilled, and the power system is stable.

Table 3 contains the CCTs estimated by the proposed algorithm, and these are compared with the CCTs obtained by the TDS using DIgSILENT Power Factory. In this test system, the sign of the percentage of variation is negative for all cases, which means that there was no overestimation of the CCT. The absolute mean of ξ is 9%.

VI. DISCUSSION

Closely methods to estimate the CCT has been found in the literature. Although [7] derive an exact equation for the first-order sensitivity of the critical clearing time without computing the DAEs of the power system, it still requires the TDS to obtain the initial critical clearing time and the post-fault trajectory. On the other hand, [14] compute the fault-on trajectory at the stability boundary to detect the critical generator and then obtain the CCT by computing the least square minimisation. Further, [15] approximates the whole power system with a single machine equivalent model, then estimates the transient stability limit by a graphical index based on the transient energy approach. While [16] proposes a non-parametric statistic scheme to evaluate the stability margin online.

TABLE 3. Results of calculation of the CCT of a fault for Test System III.

Case	Line	CCT (s)		
		TDS @ DIgSILENT Power Factory	Proposed CCT algorithm	ξ (%)
1	L02-03	0.300	0.235	−22
2	L15-16	0.160	0.145	−10
3	L16-24	0.216	0.202	−6
4	L17-18	0.280	0.269	−4
5	L17-27	0.213	0.195	−3

The main advantage of the proposed algorithm, in contrast to the algorithm proposed in [24], is that it does not need to use Hilbert-Huang techniques since these techniques require global information for the analysis [22], [23], [26]. Meanwhile, the proposed methodology only uses local temporary information, and it is suitable for online applications. Besides, this method does not use an equivalent of the power system as in [15] and [24]. Moreover, the proposed algorithm does not calculate the DAEs of the power system or use the TDS to set initial parameters, unlike [7], [14]–[16].

From the results obtained from the numerical studies, it can be noticed that the smallest CCT of a fault can be used as an index of stability since this gives a view of the global transient stability of the power system, i.e., this time represents the distance to instability.

Another aspect that is important to highlight is the computational complexity of this algorithm. The threshold and the critical clearing time estimation was performed on a 3.80 GHz AMD Ryzen 9 3900X 12-Core Processor in the MATLAB R2021a environment. For the New England test system, in [7], the overall computation time was 28 s. Meanwhile, the total computation time for the proposed algorithm is 0.98 s (including the calculation of the threshold), and for a single sliding window, the time is 0.033 s. The complexity of the proposed algorithm depends on the dimension of the measurement matrix, i.e., the number of synchronous generators in the power system.

Moreover, for verifying that the proposed algorithm is not affected by the presence of noise, the measured signals from Test System II, Case 2, are injected with noise, with a magnitude about 0.58 degrees (signal-to-noise ratio

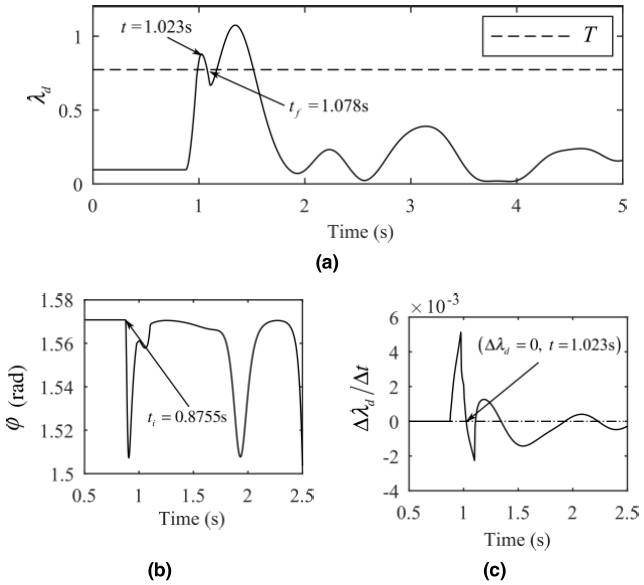

FIGURE 10. Time response of λ_d after a fault for a stable event with the presence of noise (Test System II (Case 2)): a) Magnitude of λ_d, b) Angle, φ, between λ_d and the rest of eigenvalues, c) Identification of λ_d trajectory change.

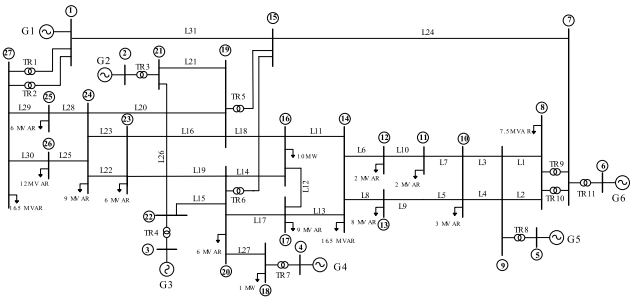

FIGURE 11. Test System I: Single-line diagram of the 6 generators and 27 buses system.

TABLE 4. Parameters of the transmission lines of Test System I.

Line	Parameters					
	R_0 (Ω)	L_0 (H)	C_0 (F)	R_0 (Ω)	L_0 (H)	C_0 (F)
L1, L2	4.855	18.099	36.334	0.755	5.954	50.464
L3, L4	8.497	31.674	63.584	1.322	10.419	88.312
L5, L7	14.638	66.651	77.829	4.100	19.546	149.671
L6, L9, L11	10.907	49.662	57.990	3.055	14.564	111.520
L8, L10, L12	7.176	32.672	38.152	2.010	9.581	73.368
L13, L25	15.499	70.572	82.407	4.342	20.696	158.475
L14, L18, L20	27.841	126.768	148.028	7.799	37.175	284.669
L15	16.387	61.085	122.627	2.549	20.094	170.315
L16, L19, L28	10.907	49.662	57.990	3.055	14.564	111.520
L17, L29, L30	22.961	104.551	122.085	6.432	30.660	234.778
L21	13.959	52.035	104.460	2.171	17.117	145.084
L22, L23	14.064	64.037	74.777	3.940	18.779	143.802
L24	71.036	0.751	2e-6	3.752	0.198	3e-6
L26	2.428	9.050	18.167	0.378	2.977	25.232
L27	6.601	30.058	35.099	1.849	8.815	67.499
L31	47.357	0.501	1e-6	2.502	0.132	2e-6

of 40 dB) [38], [39]. When the system is operating in a steady-state condition, λ_d has a small variation due to the noise (see Figure 10a) compared to the behaviour without noise (see Figure 8a). Despite this, it reflects the presence of a disturbance by having a significant change of ξ and correctly identify the moment where the disturbance starts (see Figure 10b). Otherwise, when the system has a transient response, the presence of noise in the data is considerably attenuated (see Figure 10a) such that the behaviour of λ_d is practically the same as that obtained in the case where data does not contain noise, and the λ_d trajectory change is correctly identified.

The critical cleaning time estimated by the algorithm proposed for the noise signal is 0.325 s. In comparison with the time calculated by [24], it results in a percentage of variation, ξ, equal to that obtained for the signal without noise (see Table 2). This indicates that the presence of noise does not significantly affect the performance of the proposed algorithm.

VII. CONCLUSION

The proposed algorithm for estimating the CCT of a fault showed results with acceptable precision and correctly calculates the CCT for different test systems in various scenarios. Furthermore, the percentage of variation obtained concerning the TDS method and the method proposed by [24] does not exceed 10 %, so the proposed algorithm is comparable to these methods.

However, unlike the TDS method, the proposed algorithm presents considerable advantages in contrast to other methods in which some parameters such as losses in the transmission lines, realistic models of the elements of the power system and the controls of the synchronous generators are neglected. This method does not require knowing the system parameters. The measured variables of interest contain all the information on the dynamics of the angle of the rotor of the synchronous generators. It allows the proposed algorithm to provide more realistic and accurate results. Also, the smallest CCT of a fault can be used as an index of stability since this gives a view of the global transient stability of the power system. The threshold was formulated to depend only on the stable operating condition of the power system. Further, having an analytical expression for the calculation of the threshold allows it to be adaptable.

Moreover, the effect of noise in the measured data does not affect the correct estimation of the transient stability and the calculation of the CCT. However, this effect and

other drawbacks of the measurement of data will be studied thoroughly in future research.

APPENDIX A
PARAMETERS OF THE TEST SYSTEM I

The turbine-governor system of the synchronous generators is modelled as IEEEG1, and the automatic voltage regulators are modelled as a static excitation type ST1A [40]. The single-line diagram is presented in Figure 11.

Table 6, Table 5 and Table 4 contain the parameters of the transmission lines, synchronous generators and transformers, respectively.

TABLE 5. Parameters of synchronous generators of Test System I.

Parameters	Values	
	G2, G3 and G4	G5 and G6
H (s)	4.0	4.5
R_a (pu)	0.0015	0.0015
X_0 (pu)	0.15	0.10
X_l (pu)	0.15	0.10
X_d (pu)	1.00	1.13
X_q (pu)	0.61	0.66
X'_d (pu)	0.32	0.30
X'_q (pu)	0.25	0.20
X''_d (pu)	0.25	0.20
T'_{d0} (s)	5.0	6.0
T'_{q0} (s)	0.10	0.12
T''_{d0} (s)	0.05	0.05

TABLE 6. Parameters of transformers of Test System I.

Transformer	Parameters			
	S (MVA)	V (kV)	R (pu)	X (pu)
TR1, TR2, TR5, TR6, TR9, TR10	150	400/154	0.003	0.15
TR3, TR7	46	154/13.8	0.002	0.12
TR4	25	154/6.3	0.002	0.12
TR8	65	154/10.6	0.003	0.12
TR11	175	400/14.7	0.003	0.12

REFERENCES

[1] P. Kundur, "Definition and classification of power system stability IEEE/CIGRE joint task force on stability terms and definitions," *IEEE Trans. Power Syst.*, vol. 19, no. 3, pp. 1387–1401, May 2004, doi: 10.1109/TPWRS.2004.825981.

[2] P. Kundur, N. J. Balu, and M. G. Lauby, *Power System Stability and Control*. New York, NY, USA: McGraw-Hill, 1994.

[3] Z. Wang, X. Song, H. Xin, D. Gan, and K. P. Wong, "Risk-based coordination of generation rescheduling and load shedding for transient stability enhancement," *IEEE Trans. Power Syst.*, vol. 28, no. 4, pp. 4674–4682, Nov. 2013, doi: 10.1109/TPWRS.2013.2262719.

[4] R. Zhang, Y. Xu, Z. Y. Dong, and K. P. Wong, "Post-disturbance transient stability assessment of power systems by a self-adaptive intelligent system," *IET Gener., Transmiss. Distrib.*, vol. 9, no. 3, pp. 296–305, Feb. 2015, doi: 10.1049/iet-gtd.2014.0264.

[5] J. K. Robinson, "Power system stability-computaton of critical clearing time and stability margin index," M.S. thesis, Dept. Elect. Eng., Lehigh Univ., Bethlehem, PA, USA, 1976.

[6] R. B. Eastvedt, "The need for ultra-fast fault clearing," in *Proc. 3rd Annu. Western Protective Relay Conf.*, Spokane, WA, USA, 1976.

[7] S. Sharma, S. Pushpak, V. Chinde, and I. Dobson, "Sensitivity of transient stability critical clearing time," *IEEE Trans. Power Syst.*, vol. 33, no. 6, pp. 6476–6486, Nov. 2018, doi: 10.1109/TPWRS.2018.2854650.

[8] Z. Wang, A. Girgis, V. Aravnthan, and E. Makram, "Wide area power system transient stability assessment using catastrophe theory method and synchrophasors," in *Proc. IEEE Power Energy Soc. Gen. Meeting*, Jul. 2011, pp. 1–7, doi: 10.1109/PES.2011.6039022.

[9] H. Zhou, F. Tang, J. Jia, and X. Ye, "The transient stability analysis based on WAMS and online admittance parameter identification," in *Proc. IEEE Eindhoven PowerTech*, Jun. 2015, pp. 1–6, doi: 10.1109/PTC.2015.7232544.

[10] L. G. W. Roberts, A. R. Champneys, K. R. W. Bell, and M. di Bernardo, "Analytical approximations of critical clearing time for parametric analysis of power system transient stability," *IEEE J. Emerg. Sel. Topics Circuits Syst.*, vol. 5, no. 3, pp. 465–476, Sep. 2015, doi: 10.1109/JETCAS.2015.2467111.

[11] T. L. Vu, S. M. A. Araifi, M. S. El Moursi, and K. Turitsyn, "Toward simulation-free estimation of critical clearing time," *IEEE Trans. Power Syst.*, vol. 31, no. 6, pp. 4722–4731, Nov. 2016, doi: 10.1109/TPWRS.2016.2523265.

[12] C. Dong, H. Jia, T. Jiang, L. Bai, Q. Hu, L. Wang, and Y. Jiang, "Effective method to determine time-delay stability margin and its application to power systems," *IET Gener., Transmiss. Distrib.*, vol. 11, no. 7, pp. 1661–1670, May 2017, doi: 10.1049/iet-gtd.2016.0953.

[13] S. Gupta, F. Kazi, S. Wagh, and N. Singh, "Analysis and prediction of vulnerability in smart power transmission system: A geometrical approach," *Int. J. Electr. Power Energy Syst.*, vol. 94, pp. 77–87, Jan. 2018, doi: 10.1016/j.ijepes.2017.06.033.

[14] N. Yorino, A. Priyadi, H. Kakui, and M. Takeshita, "A new method for obtaining critical clearing time for transient stability," *IEEE Trans. Power Syst.*, vol. 25, no. 3, pp. 1620–1626, Aug. 2010, doi: 10.1109/TPWRS.2009.2040003.

[15] A. Shamisa and M. Karrari, "Model free graphical index for transient stability limit based on on-line single machine equivalent system identification," *IET Gener., Transmiss. Distrib.*, vol. 11, no. 2, pp. 314–321, Jan. 2017, doi: 10.1049/iet-gtd.2015.1539.

[16] T. Liu, Y. Liu, L. Xu, J. Liu, J. Mitra, and Y. Tian, "Non-parametric statistics-based predictor enabling online transient stability assessment," *IET Gener., Transmiss. Distrib.*, vol. 12, no. 21, pp. 5761–5769, Nov. 2018, doi: 10.1049/iet-gtd.2018.5802.

[17] J. J. Gerbrands, "On the relationships between SVD, KLT and PCA," *Pattern Recognit.*, vol. 14, nos. 1–6, pp. 375–381, Jan. 1981, doi: 10.1016/0031-3203(81)90082-0.

[18] G. Kerschen, J.-C. Golinval, A. F. Vakakis, and L. A. Bergman, "The method of proper orthogonal decomposition for dynamical characterization and order reduction of mechanical systems: An overview," *Nonlinear Dyn.*, vol. 41, nos. 1–3, pp. 147–169, Aug. 2005, doi: 10.1007/s11071-005-2803-2.

[19] Carson W. Taylor, *Power System Voltage Stability*. New York, NY, USA: McGraw-Hill, 1994.

[20] J. M. Lim and C. L. DeMarco, "SVD-based voltage stability assessment from phasor measurement unit data," *IEEE Trans. Power Syst.*, vol. 31, no. 4, pp. 2557–2565, Jul. 2016, doi: 10.1109/TPWRS.2015.2487996.

[21] A. R. Messina and V. Vittal, "Extraction of dynamic patterns from wide-area measurements using empirical orthogonal functions," *IEEE Trans. Power Syst.*, vol. 22, no. 2, pp. 682–692, May 2007, doi: 10.1109/TPWRS.2007.895157.

[22] P. Esquivel, E. Barocio, M. A. Andrade, and F. Lezama, "Complex empirical orthogonal function analysis of power system oscillatory dynamics," in *Inter-Area Oscillations Power System*. Boston, MA, USA: Springer, 2009, pp. 159–187.

[23] A. R. Messina, M. A. Andrade, J. H. Hernandez, and R. Betancourt, "Analysis and characterization of power system nonlinear oscillations using Hilbert spectral analysis," *Open Electr. Electron. Eng. J.*, vol. 1, no. 1, pp. 1–8, Dec. 2007, doi: 10.2174/1874129000701010001.

[24] A. Paul and N. Senroy, "Critical clearing time estimation using synchrophasor data-based equivalent dynamic model," *IET Gener., Transmiss. Distrib.*, vol. 9, no. 7, pp. 609–614, Apr. 2015, doi: 10.1049/iet-gtd.2014.0519.

[25] E. Barocio, B. C. Pal, D. Fabozzi, and N. F. Thornhill, "Detection and visualization of power system disturbances using principal component analysis," in *Proc. Symp. Bulk Power Syst. Dyn. Control Optim., Secur. Control Emerg. Power Grid*, Aug. 2013, pp. 1–10, doi: 10.1109/IREP.2013.6629374.

[26] M. A. Andrade, A. R. Messina, C. A. Rivera, and D. Olguin, "Identification of instantaneous attributes of torsional shaft signals using the Hilbert transform," *IEEE Trans. Power Syst.*, vol. 19, no. 3, pp. 1422–1429, Aug. 2004, doi: 10.1109/TPWRS.2004.829664.
[27] E. Gómez, E. Vázquez, N. Acosta, and M. A. Andrade, "Independent estimation of generator clustering and islanding conditions in power system with microgrid and inverter-based generation," in *Wide Area Power Systems Stability, Protection, and Security* (Power Systems). Cham, Switzerland: Springer, 2021, pp. 523–553.
[28] J. M. Lim and C. L. DeMarco, "Power system network partitioning for SVD based information retrieval using PMU data," in *Proc. IEEE PES Gen. Meeting/Conf. Expo.*, Jul. 2014, pp. 1–5, doi: 10.1109/PESGM.2014.6939514.
[29] X. He, Q. Ai, R. C. Qiu, W. Huang, L. Piao, and H. Liu, "A big data architecture design for smart grids based on random matrix theory," *IEEE Trans. Smart Grid*, vol. 8, no. 12, pp. 674–686, Mar. 2017, doi: 10.1109/TSG.2015.2445828.
[30] D. Ma, X. Hu, and H. Zhang, "A hierarchical event detection method based on spectral theory of multidimensional matrix for power system," *IEEE Trans. Syst. Man, Cybern. Syst.*, vol. 51, no. 4, pp. 2173–2186, Apr. 2021, doi: 10.1109/TSMC.2019.2931316.
[31] G. Strang, *Linear Algebra and its Applications*, 4th ed. Boston, MA, USA: Cengage Learning, 2006.
[32] G. H. Golub and C. F. Van Loan, *Matrix Computations*, 3rd ed. Baltimore, MD, USA: Johns Hopkins Univ. Press, 1996.
[33] H. Khalil, *Nonlinear Systems*, 3rd ed. London, U.K.: Pearson, 2001.
[34] A. Prince, N. Senroy, and R. Balasubramanian, "Targeted approach to apply masking signal-based empirical mode decomposition for mode identification from dynamic power system wide area measurement signal data," *IET Gener., Transmiss. Distrib.*, vol. 5, no. 10, p. 1025, 2011, doi: 10.1049/iet-gtd.2011.0057.
[35] T. L. Vu and K. Turitsyn, "Lyapunov functions family approach to transient stability assessment," *IEEE Trans. Power Syst.*, vol. 31, no. 2, pp. 1269–1277, Mar. 2016, doi: 10.1109/TPWRS.2015.2425885.
[36] S. Paudyal, G. Ramakrishna, and M. S. Sachdev, "Application of equal area criterion conditions in the time domain for out-of-step protection," *IEEE Trans. Power Del.*, vol. 25, no. 2, pp. 600–609, Apr. 2010, doi: 10.1109/TPWRD.2009.2032326.
[37] M. A. Pai, *Energy Function Analysis for Power System Stability*. Cham, Switzerland: Springer, 1989.
[38] *IEEE Standard for Synchrophasor Measurements for Power Systems*, Standard C37.118.1-2011, 2011.
[39] M. Brown, M. Biswal, S. Brahma, S. J. Ranade, and H. Cao, "Characterizing and quantifying noise in PMU data," in *Proc. IEEE Power Energy Soc. Gen. Meeting (PESGM)*, Jul. 2016, pp. 1–5, doi: 10.1109/PESGM.2016.7741972.
[40] *IEEE Recommended Practice for Excitation System Models for Power System Stability Studie*, Standard 421.5-2016, 2016.

MARTHA N. ACOSTA received the B.Sc. degree in mechanical and electrical engineering and the master's degree in electrical engineering from the Universidad Autónoma de Nuevo León, Nuevo León, Mexico, in 2015 and 2017, respectively, where she is currently pursuing the Ph.D. degree in electrical engineering in conjunction with the University of South-Eastern Norway. Her research interest includes developing intelligent frequency control methodologies for the secure operation of the modern power system considering the integration of power converters-based technologies.

EDGAR GÓMEZ received the B.Sc. degree in electrical engineering from the Tuxtla Gutiérrez Institute of Technology, Chiapas, Mexico, in 2014, and the M.Sc. degree in electrical engineering from the School of Mechanical and Electrical Engineering, Universidad Autónoma de Nuevo León, Mexico, in 2018, where he is currently pursuing the Ph.D. degree in electrical engineering. His research interests include power system stability and control and grid integration of renewables.

FRANCISCO GONZALEZ-LONGATT (Senior Member, IEEE) is currently a Full Professor of electrical power engineering with the Institutt for elektro, IT og kybernetikk, Universitetet i Sørøst-Norge, Norway. He has prolific research productivity including several industrial research projects and consultancy worldwide. Also, he is the author or editor of several books (Spanish and English). His research interest includes innovative (operation/control) schemes to optimize the performance of future energy systems. He is a member of The Institution of Engineering and Technology–The IET (U.K.) and a member of the International Council on Large Electric Systems–CIGRE. He received the Professional Recognition as a Fellow of the Higher Education Academy (FHEA), in January 2014. He is an associate editor in several journals with an impressive track record on scientific publications. He is the Vice-President of Venezuelan Wind Energy Association.

MANUEL A. ANDRADE (Member, IEEE) received the B.Sc. degree in electrical engineering from Saltillo Institute of Technology, Saltillo, Mexico, in 2000, and the M.Sc. and Ph.D. degrees in electrical engineering from the Center for Research and Advanced Studies, National Polytechnic Institute, Guadalajara, Mexico, in 2002 and 2007, respectively. He is currently an Associate Professor with the Universidad Autónoma de Nuevo Leon, Monterrey, México, where he joined, in 2007.

ERNESTO VÁZQUEZ (Member, IEEE) received the B.Sc. degree in electronic and communication engineering and the M.Sc. and Ph.D. degrees in electrical engineering from the Universidad Autónoma de Nuevo León (UANL), Mexico, in 1988, 1991, and 1994, respectively. Since 1996, he has been a Research Professor of electrical engineering with the UANL. In 2001 and 2011, he conducted a research stay with the University of Manitoba and the University of Alberta, Canada, where he was working in traveling-wave protection algorithms and fault-resistance estimation, respectively.

EMILIO BAROCIO (Senior Member, IEEE) received the M.E. degree in electrical engineering from the University of Guadalajara, Guadalajara, México, in 1998, and the Ph.D. degree in electrical engineering from CINVESTAV, Guadalajara, in 2003. He is currently a Researcher/Professor with the Department of Mechanical and Electrical Engineering, University of Guadalajara. He was a recipient of the Arturo Rosenblueth Award for the Best Ph.D. Thesis on Science and Technology of México in 2003. He was distinguished with the Marie-Curie Incoming International Fellowship at Imperial College of London, in 2013. He was also a recipient of with the IEEE Power and Energy Society's Power System Dynamic Performance Committee Prize Paper Awards in 2018.